VI-F Photoionization and Photodissociation Dynamics Studied by Electron and Fluorescence Spectroscopy

Molecular photoionization is a major phenomenon in vacuum UV excitation and provides a large amount of information on fundamental electron-core interactions in molecules. Especially, neutral resonance states become of main interest, since they often dominate photoabsorption cross sections and lead to various vibronic states which are inaccessible in direct ionization. We have developed a versatile machine for photoelectron spectroscopy in order to elucidate dynamical aspects of superexcited states such as autoionization, resonance Auger decay, predissociation, vibronic couplings, and internal conversion. Two-dimensional photoelectron spectroscopy, allows us to investigate superexcited states in the valence excitation region of acetylene, nitric oxide, carbonyl sulfide, sulfur dioxide and so on. In a two-dimensional photoelectron spectrum (2D-PES), the photoelectron yield is measured as a function of both photon energy $E_{h\nu}$ and electron kinetic energy E_k (binding energy). The spectrum, usually represented as a contour plot, contains rich information on photoionization dynamics.

Photofragmentation into ionic and/or neutral species is also one of the most important phenomena in the vacuum UV excitation. In some cases, the fragments possess sufficient internal energy to de-excite radiatively by emitting UV or visible fluorescence. It is widely accepted that fluorescence spectroscopy is an important tool to determine the fragments and to clarify the mechanisms governing the dissociation processes of diatomic and polyatomic molecules. For several years we have concentrated upon fluorescence spectroscopy of H_2O in the photon energy region of 15–55 eV.

VI-F-1 Dissociation Mechanism of H_2O into $OH^+(\tilde{A}^3\Pi_\Omega)$ + H(n = 1) Manifested by Ultraviolet Dispersed Spectroscopy

MITSUKE, Koichiro

The photofragmentation of H_2O has been studied by fluorescence spectroscopy at photon energies between $h\nu$ = 16.9–54.5 eV. The primary photon beam was monochromatized undulator radiation supplied from BL3A2 of the UVSOR facility. The fluorescence in the wavelength range of 280–720 nm was dispersed with an imaging spectrograph.[1] Figure 1 shows the fluorescence excitation spectrum for the (0,0) vibrational band of the $OH^+(\tilde{A}^3\Pi_\Omega \rightarrow \tilde{X}_3\Sigma^-)$ transition. The intensity shows a slow onset at 25.5 ± 0.3 eV. This value is much higher than the dissociation limit of 21.5 eV and can be interpreted in terms of a highly repulsive potential energy surface of the excited H_2O^+ state along the dissociation coordinate. The correlation diagram of H_2O^+ proposed by Appell and Durup[2] predicts that the $OH^+(\tilde{A}^3\Pi_\Omega)$ + H(n = 1) limit correlates with a 2-hole 1-particle $^2A_1$ state of H_2O^+ with the electronic configuration of $[(1b_1)^{-2}(4a_1)^1]$. This doubly excited $H_2O^+(^2A_1)$ state was reported to be located at 27.6 ± 1 eV with respect to $H_2O(\tilde{X}^1A_1)$ in the Franck-Condon region. This vertical ionization energy rationalizes the present observation that the $OH^+(\tilde{A}^3\Pi_\Omega \rightarrow \tilde{X}^3\Sigma^-)$ band system begins to appear at $h\nu$ = 25.5 eV.

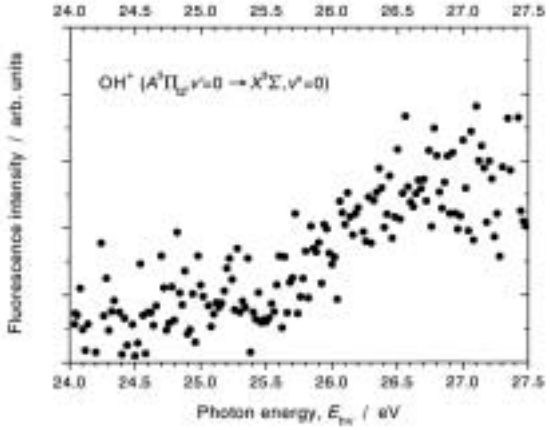

Figure 1. Fluorescence excitation spectrum for the (0,0) vibrational band of the $OH^+(\tilde{A}^3\Pi_\Omega \rightarrow \tilde{X}^3\Sigma^-)$ transition. The resolution of the synchrotron radiation was 2.4 Å.

References

1) K. Mitsuke, *J. Chem. Phys.* **117**, 8334–8340 (2002).
2) J. Appell and J. Durup, *Int. J. Mass Spectrom. Ion Phys.* **10**, 247–265 (1972/73).

VI-F-2 Autoionization of the Rydberg States Converging to $HI^+(A\,^2\Sigma^+_{1/2})$ below $h\nu$ = 12.7 eV

HIKOSAKA, Yasumasa[1]; MITSUKE, Koichiro
([1]Inst. Mater. Struct. Sci.)

[*J. Chem. Phys.* submitted]

Two-dimensional photoelectron spectroscopy of hydrogen iodide has been performed in the $E_{h\nu}$ range of 11.10–14.85 eV, in order to clarify autoionization mechanisms of the Rydberg states $HI^*(R_A)$ converging to $HI^+(\tilde{A}^2\Sigma^+_{1/2})$. The 2D-PES exhibits extensive vibrational excitation of $HI^+(\tilde{X}^2\Pi_{3/2}, v^+)$ over a $E_{h\nu}$ region from ~ 12 to 13.6 eV. The v^+ excitation below 12.7 eV is attributable to autoionizing features of the $5d\pi$ $HI^*(R_A)$ state. The potential energy curves of HI* and HI^+ are illustrated in Figure 1, where the curves of HI^+ are adopted from the literature.[1] Superexcitation and subsequent autoionization is usually governed by the Franck-Condon principle. Since the wave functions for excited vibrational levels have large amplitudes near

the potential wall, superexcitation into $5d\pi$ HI*(R_A) affords population to a few vibrational levels whose classical turning points at the repulsive branch of $5d\pi$ HI*(R_A) are included within the Franck-Condon region for transitions from HI($\tilde{X}^1\Sigma^+$). Then autoionization of these levels occurs either at near the repulsive branch or at the attractive branch, unless the lifetime with respect to autoionization is much shorter than the vibrational period of the $5d\pi$ state. The extensive vibrational excitation at $E_{h\nu}$ < 12.7 eV can be accounted for by autoionization at the attractive branch.

Reference

1) A. J. Cormack, *et al.*, *Chem. Phys.* **221**, 175–188 (1997).

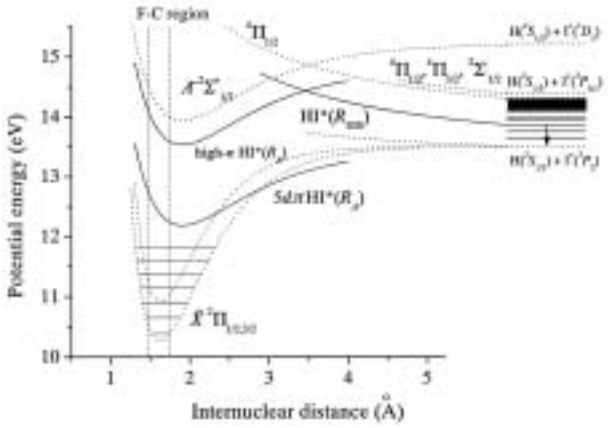

Figure 1. Schematic diagram for the potential energy curves of HI and HI^+. The solid and dashed lines designate the Rydberg and ionic states, respectively. The potential energy curves of HI*(R_A) states are assumed to have the same shape as those of $HI^+(\tilde{A}^2\Sigma^+_{1/2})$. The term values used for the $5d\pi$ and high-n Rydberg states are 1.76 and 0.44 eV, respectively. The Franck-Condon region is located between the two dashed vertical lines.

VI-F-3 Autoionization and Predissociation of the Rydberg States Converging to $HI^+(\tilde{A}^2\Sigma^+_{1/2})$ at $h\nu$ = 13.2–13.6 eV

HIKOSAKA, Yasumasa[1]; MITSUKE, Koichiro
([1]Inst. Mater. Struct. Sci.)

The 2D-PES of HI at $E_{h\nu}$ = 13.2–13.6 eV has been closely studied to understand dynamical properties on autoionization and predissociation of HI*(R_A) (see also Theme VI-F-2). The v^+ distribution of $HI^+(\tilde{X}^2\Pi_{3/2})$ shows an interesting left-side up pattern up to $v^+ \sim 12$. Namely, the relative population for a given v^+ reaches a maximum at $E_{h\nu} = E_{h\nu}^{max}$ whose value increases with increasing v^+. At first sight one would presume that this vibrational pattern results from autoionization of high-n HI*(R_A) Rydberg states with n » 5.

Figure 1 shows the constant-ionic-state (CIS) spectra for v^+ = 0–3 of $HI^+(\tilde{X}^2\Pi_{3/2})$ extracted from the 2D-PES. Panel (a) shows a broad resonance peak due to autoionization of $5d\pi$ HI*(R_A). With increasing v^+ the spectral features spread from ~ 12.0 to ~ 13.3 eV and become complicated as seen from the other three Panels. At $v^+ \geq 3$ the whole resonance splits into two broad peaks. The peak lying at higher energy shifts its maximum position from ~ 13.1 eV at v^+ = 3 to ~ 13.5 eV at v^+ = 12, being consistent with the left-side up pattern. At $E_{h\nu}$ = 13.2–13.6 eV, the integrated intensity for v^+ = 1 calculated from Figure 1(a) is no more than 4% of that for v^+ = 0. This ratio is much smaller than that at $E_{h\nu}$ = 12.2–12.7 eV, which implies that simple autoionization of the high-n HI*(R_A) states occur less efficiently than their conversion into predissociating repulsive states HI*(R_{Dis}). Then there is a probability that the system is converted from HI*(R_{Dis}) to low-n HI*(R_A) through avoided curve crossings. Autoionization of low-n HI*(R_A) states, such as the $5d\pi$ state; produced by double conversion can provide populations of HI^+ ($\tilde{X}^2\Pi_{3/2,1/2}$) at higher v^+ than expected from the Franck-Condon factors between HI($\tilde{X}^1\Sigma^+$) and HI*(R_A). From the relation between the potential energy curves of low-n HI*(R_A) and $HI^+(\tilde{X}^2\Pi_{3/2})$, autoionization can proceed mostly from the repulsive branch (see Figure 1 in Theme VI-F-2). The higher the n value of the primary high-n HI*(R_A) state becomes, the more the low-n HI*(R_A) state resulting from double conversion is vibrationally excited. Consequently, autoionizing transition occurs at a shorter nuclear distance and the final vibrational distribution of $HI^+(\tilde{X}^2\Pi_{3/2,1/2})$ shifts to higher v^+. The left-side up pattern at $E_{h\nu}$ = 13–13.7 eV in the 2D-PES obviously supports this expectation.

Reference

1) Y. Hikosaka and K. Mitsuke, *J. Chem. Phys.* submitted.

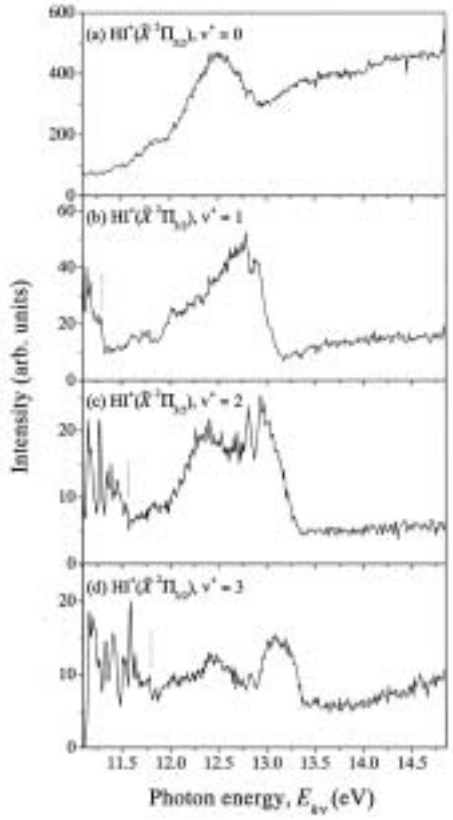

Figure 1. CIS spectra for the formation of v^+ = 0–3 vibrational levels of $HI^+(\tilde{X}^2\Pi_{3/2})$, which are extracted from the 2D-PES. The ionization energies for the v^+ = 1, 2 and 3 levels of $HI^+(\tilde{X}^2\Pi_{1/2})$ are indicated by the dotted lines in the spectra for v^+ = 1, 2 and 3, respectively.

VI-G Vacuum UV Spectroscopy Making Use of a Combination of Synchrotron Radiation and Laser

There is a growing interest in combining synchrotron radiation (SR) with the laser, since high resolution or ultrafast lasers are expected to open a new field for studies on dynamical behaviors of excited molecules in the VUV or soft X-ray region. Nevertheless, only a few attempts have been made on pump-probe experiments of gas-phase molecules using SR and a laser: photoelectron spectroscopy of atomic iodine produced from I_2 (Nahon *et al.*, 1990, 1991), photoelectron spectroscopy of N_2 and HCN produced from *s*-tetrazine (Nahon *et al.*, 1992), and photoionization of atomic iodine produced from CH_3I (Mizutani *et al.*, 1997). In UVSOR we have developed ultraviolet laser system which synchronizes precisely with the SR pulses from the storage ring to take maximum advantage of the features of the laser, *i.e.* its excellent spectral and temporal resolution, we employed the laser in detecting and analyzing products resulting from VUV or soft X-ray photoexcitation. The following combination studies have been performed: (1) two-photon ionization of helium atoms studied as the prototype of the time-resolved experiment (Mizutani *et al.*, 1997), (2) laser induced fluorescence (LIF) excitation spectroscopy of $N_2^+(X\ ^2\Sigma_g^+)$ ions or $CN(X\ ^2\Sigma^+)$ radicals produced by SR photoionization of N_2, N_2O, or CH_3CN (Mizutani *et al.*, 1998; Mitsuke *et al.*, 1998, 2001). This year another combination work commences as a new project, that is, SR photodissociation of vibrationally excited molecules prepared with irradiation of visible or infrared single frequency laser.

VI-G-1 Development of the Laser–SR Combination System for Photodissociation Studies of Highly Vibrationally Excited Molecules

MITSUKE, Koichiro

It is possible that the initial vibrational excitation in a molecule influences the chemical branching, if two different photodissociation channels are accessible. Much attention has been focused on the pioneering work of Crim and his collaborators,[1] who could accomplish the selective bond-breaking of heavy water, HOD. Very recently, Akagi and coworkers[2] reported that deuterized ammonia NHD_2 in the fourth N–H stretching overtone preferentially photodissociates into the ND_2 + H channel. In these two studies UV lasers were employed for vibrationally mediated photodissociation.

Instead, we are planning to use synchrotron radiation (SR) to promote vibrationally excited molecules to electronically excited states in the vacuum UV region. The main objectives are as follows: (1) Elucidating the properties of dissociative states by sampling a wide range of their potential energy surfaces, such as dynamics determining the final-state distributions of the products, nonadiabatic transitions on dissociation, and assignments and characterization of unknown multiply-excited states produced by Auger decay from core-excited states. (2) Aiming at more universal "vibrational state-specific" rupture of chemical bonds, which could be realized by changing the overlap between the wave-fucntions of the upper-state continuum and that of the ground state.

References

1) R. L. Vander Wal, J. L. Scott and F. F. Crim, *J. Chem. Phys.* **92**, 803–805 (1990).
2) H. Akagi, K. Yokoyama and A. Yokoyama, *J. Chem. Phys.* **118**, 3600–3611 (2003).

VI-G-2 Photodissociation of Vibrationally Excited H_2O in the $4\nu_{O-H}$ Region into $OH^+(X^3\Sigma^-)$ + H(n = 1)

MITSUKE, Koichiro; KOU, Junkei; MORI, Takanori

We have searched appropriate excited states through which photodissociation of vibrationally excited molecules can be investigated, on the basis of the correlation diagram in Figure 1 that we proposed in the dispersed fluorescence study for the extreme UV photoionization of H_2O.[1] First, we tackled the two $^2A_1$ states which correlate with the $OH^+(A^3\Pi_\Omega)$ + H(n = 1) and OH $(A^2\Sigma^+)$ + H^+ limits. Since the two states are highly repulsive, it is possible that significant decrease in the appearance energy is observed for the formation of $OH^+(A^3\Pi_\Omega)$ or $OH(A^2\Sigma^+)$ from vibrationally excited molecules. Here, spontaneous emission from these photofragments are detected.

A continuous titanium-sapphire laser was used in the wavenumber range between 13814–13819 cm^{-1}, with its bandwidth of 4×10^{-4} cm^{-1}. This energy range corresponds to excitation of the third O–H stretching overtone of water. However, when the visible laser was introduced together with SR, no additional peak feature of emission bands was detected in the dispersed spectra. Then we shifted the target to the dissociation channel of $OH^+(X^3\Sigma^-)$ + H(n = 1). The OH^+ ion was detected using mass spectrometry at SR photon energies near the dissociation threshold of 18.05 eV with respect to the neutral ground state. The difference between the normalized signal ion counts with and without the visible laser appears to exhibit multi-modal reflection structures due to the nodes of the vibrational wave function of the $4\nu_{O-H}$ stretch overtone of H_2O.

Reference

1) K. Mitsuke, *J. Chem. Phys.* **117**, 8334–8340 (2002).

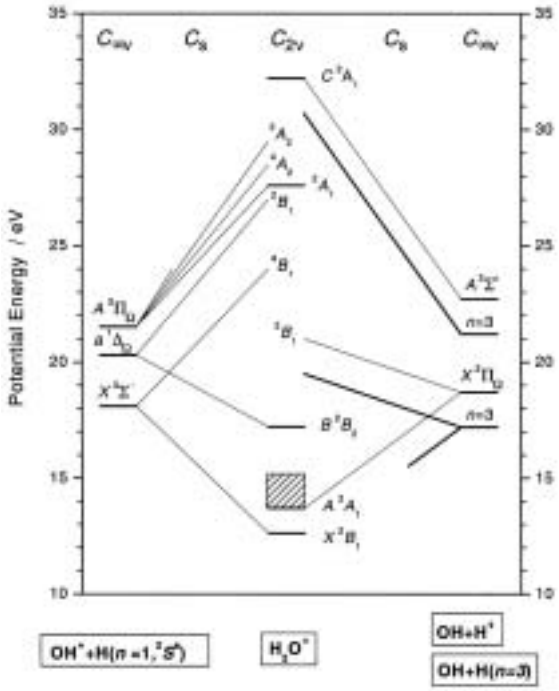

Figure 1. Correlation diagram between H_2O^+ and $OH^+ + H$ and between H_2O^+ and $OH + H^+$.

VI-H Extreme UV Photoionization Studies of Polyatomic Molecules and Fullerenes by Employing a Grazing-Incidence Monochromator

On the beam line BL2B2 in UVSOR a grazing incidence monochromator has been constructed which supplies photons in the energy region from 20 to 200 eV [M. Ono, H. Yoshida, H. Hattori and K. Mitsuke, *Nucl. Instrum. Methods Phys. Res., Sect. A* **467-468**, 577–580 (2001)]. This monochromator has bridged the energy gap between the beam lines BL3B and BL4B, thus providing for an accelerating demand for the high-resolution and high-flux photon beam from the research fields of photoexcitation of inner-valence electrons, *L*-shell electrons in the third-row atom, and 4*d* electrons of the lanthanides.

Since 2001 we have tried taking photoion yield curves of fullerenes. Geometrical structures and electronic properties of fullerenes have attracted widespread attention because of their novel structures, novel reactivity, and novel catalytic behaviors as typical nanometer-size materials. Moreover, it has been emphasized that the potential for the development of fullerenes to superconductors ($T_c \sim 50$ K) and strong ferromagnetic substances is extremely high. In spite of such important species spectroscopic information is very limited in the extreme UV region, which has been probably due to difficulties in obtaining enough amount of sample. The situation has been rapidly changed in these few years, since the techniques of syntheses, isolation, and purification have been advanced so rapidly that appreciable amount of fullerenes is obtainable from several distributors in Japan.

VI-H-1 Anisotropy of Fragment Ions from SF_6 by Photoexcitation between 23 and 210 eV

ONO, Masaki[1]; MITSUKE, Koichiro
([1]Louisiana State Univ.)

[*Chem. Phys. Lett.* **366**, 595–600 (2002)]

The anisotropy of the ionic photofragments produced from SF_6 has been measured using synchrotron radiation in the range of 23–210 eV. Despite the highly symmetrical molecule a strong anisotropy is observed below ~ 35 eV. The behavior of the asymmetry parameter involving all the fragment ions has been interpreted by simulation using partial oscillator strengths for the formation of individual species. Only SF_5^+ ions produced via superexcited states of valence type are assumed to have an anisotropic angular distribution. The observed decrease in the asymmetry parameter with increasing photon energy can be ascribed to the dominance of direct photoionization and the decrease in the branching ratio for SF_5^+ formation.

VI-H-2 Kinetic Energy Distribution and Anisotropy of Fragment Ions from SF_6 by Photoexcitation of a Sulfur 2*p*-Electron

ONO, Masaki[1]; MITSUKE, Koichiro
([1]Louisiana State Univ.)

[*Chem. Phys. Lett.* in press]

The kinetic energy (KE) distribution and asymmetry parameter β have been studied for photofragmentation of SF_6 near the sulfur 2*p* ionization edges at 170–208 eV by using synchrotron radiation. The relative yield of fast ions with KE > 5 eV is larger in the post-edge than in the pre-edge region (see Figure 1), whereas β of such ions is lower in the post-edge region. The β curve shows a sudden drop from 0.06–0.07 to zero near the edges and remains constant thereafter. These results are ascribed to *LVV* Auger decay occurring above the edges leading to SF_6^{2+} and SF_6^{3+} transiently. At KE > 2 eV the distribution curve for the S $2p \rightarrow 6a_{1g}$ resonance transition behaves in the same manner as that for the valence-electron ionization at 170 eV. This agreement, together with a similarity in β, suggests that the S $2p \rightarrow 6a_{1g}$ resonance and valence-electron ionization suffer similar formation pathways leading to ions with high KE.

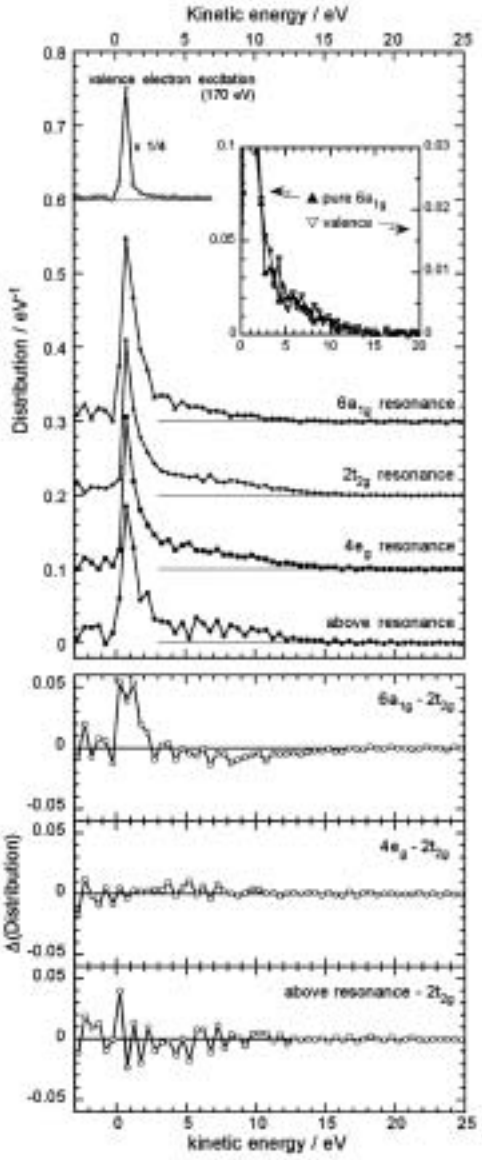

Figure 1. Upper panel: Kinetic energy distributions for sheer S 2*p*-electron excitation after subtracting the contributions of valence-electron photoionization. Inset shows expansion of the two distributions for the $6a_{1g}$ resonance at $h\nu$ = 173.5 eV and valence-electron ionization at 170 eV. Lower panel: Differences in distribution between the $2t_{2g}$ resonance and one of the three excitation energies (the $6a_{1g}$, $4e_g$ resonance and above the resonance).

VI-H-3 Molecular- and Atomic-Like Photoionization of C_{60} in the Extreme Ultraviolet

KOU, Junkei; MORI, Takanori; ONO, Masaki[1]; HARUYAMA, Yusuke[2]; KUBOZONO, Yoshihiro[3]; MITSUKE, Koichiro
([1]Louisiana State Univ.; [2]Okayama Univ.; [3]IMS and Okayama Univ.)

[*Chem. Phys. Lett.* **374**, 1–6 (2003)]

Photoion yield spectra of C_{60} in the gas phase have been measured from 23 to 180 eV by using synchrotron radiation. Two peaks at 26 and 34 eV and a flat area ranging from 40 to 50 eV are newly observed in the higher energy side of the giant resonance at ~ 20 eV, as shown in Figure 1. These features are assigned as resulting from the shape resonance on photoionization of valence electrons of C_{60} with large orbital angular momenta: the ionized electron is temporarily trapped inside a centrifugal barrier. Above ~ 50 eV the yield curve shows a steady decrease with increasing photon energy like the photoabsorption cross section of atomic carbon. Thus, the spectrum is considered to be determined by photoionization of the 2*s* orbitals of the carbon atoms.

Reference

1) P. Colavita, *et al.*, *Phys. Chem. Chem. Phys.* **3**, 4481–4487 (2001).

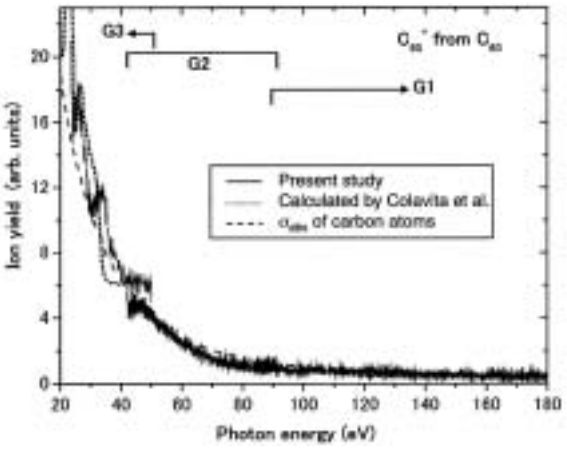

Figure 1. Solid curves: photoion yield of C_{60}^+ from C_{60} (present study). The dotted and dashed curves indicate the calculated photoabsorption cross sections of C_{60} and sixty carbon atoms, respectively, taken from Reference 1).

VI-H-4 Development of a Photoionization Spectrometer for Accurate Ion Yield Measurements from Gaseous Fullerenes

MORI, Takanori; KOU, Junkei; ONO, Masaki[1]; HARUYAMA, Yusuke[2]; KUBOZONO, Yoshihiro[3]; MITSUKE, Koichiro
([1]Louisiana State Univ.; [2]Okayama Univ.; [3]IMS and Okayama Univ.)

[*Rev. Sci. Instrum.* **74**, 3769–3773 (2003)]

A photoionization spectrometer has been developed for measuring the ion yields for fullerenes in the photon energy range of 23–200 eV (see Figure 1). Gaseous fullerenes were supplied from a high-temperature oven, ionized by irradiation of monochromatized synchrotron radiation and detected after analysis with a time-of-flight mass spectrometer. The fluxes of the synchrotron radiation and fullerene beams were monitored concurrently with the acquisition of the ion signal counts in order to obtain reliable photoionization efficiency curves. The performance of the apparatus was examined by measuring the efficiency curve of C_{60}^+ produced from C_{60}. The spectrum demonstrated better statistics than the previous results in the same photon energy region. Three distinct features were newly observed in the higher energy side of the prominent resonance at ~ 20 eV.

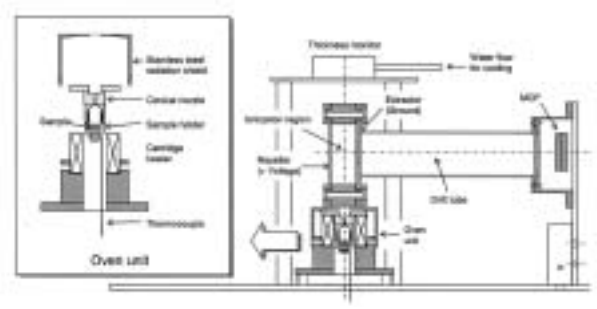

Figure 1. Apparatus of the photoionization spectrometer and an expansion of the oven unit.

VI-H-5 Production of Doubly Charged Ions in Valence Photoionization of C_{60} and C_{70} at $h\nu$ = 25–150 eV

KOU, Junkei; MORI, Takanori; S. V. K. Kumar[1]; HARUYAMA, Yusuke[2]; KUBOZONO, Yoshihiro[3]; MITSUKE, Koichiro
([1]IMS and Tata Inst. Fund. Res.; [2]Okayama Univ.; [3]IMS and Okayama Univ.)

[*J. Chem. Phys.* submitted]

Relative partial photoionization cross sections for production of singly and doubly charged ions of C_{60} and C_{70} have been measured at $h\nu$ = 25–150 eV. Figure 1 shows the photoionization yield curves of C_{60} for the formation of C_{60}^{n+} (n = 1 and 2). Since the yields for multiply charged ions with $n \geq 3$ are not significant in this energy region, one can regard the composite spectrum obtained by summing up the yields for C_{60}^+ and C_{60}^{2+} as the total photoionization yield of C_{60} or, to a good approximation, the total photoabsorption cross section of C_{60}. There are three peaks at $h\nu$ = 26, 34, and 49 eV in the composite spectrum. The total photoabsorption spectrum theoretically determined by Colavita and cowokers[1)] is depicted by the dotted curve in Figure 1. A comparison of the present total photoionization yield with the reported photoabsorption spectrum shows a large disagreement, probably because of the contribution of C_{60}^{2+} produced through the mechanism that has not been taken into account[1)] in the *ab initio* calculations. The most probable pathway to produce C_{60}^{2+} is considered to be spectator Auger decay of shape resonance states followed by cascade or electron tunneling, because there are many shape resonance states at various photon energies. In contrast, resonace Auger processes have been disregarded in the calculations.[1)] The partial and total photoionzation yield curves of C_{70} are similar to those of C_{60}. Ratio of the yields of C_{60}^{2+}/C_{60}^+ and C_{70}^{2+}/C_{70}^+ are found to be larger than unity at $h\nu$ > 50 eV. The observed yield curves and ratios quite differ from those reported in the electron impact ionization of C_{60} and C_{70}.

Reference

1) P. Colavita, *et al*., *Phys. Chem. Chem. Phys.* **3**, 4481–4487 (2001).

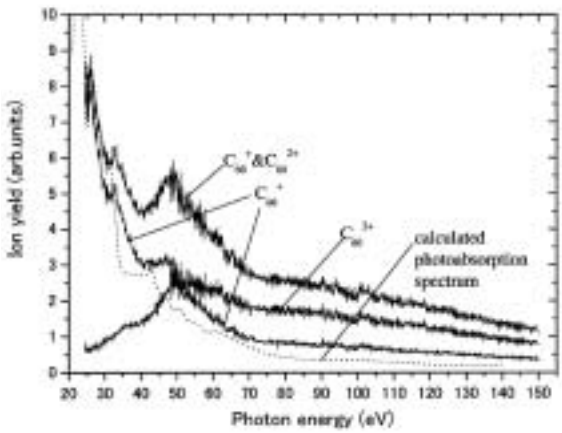

Figure 1. Partial and total photoionization yield curves of C_{60}.